Supplement of Nat. Hazards Earth Syst. Sci., 23, 1409–1423, 2023
https://doi.org/10.5194/nhess-23-1409-2023-supplement

Natural Hazards and Earth System Sciences
Open Access

Supplement of

An assessment of short–medium-term interventions using CAESAR-Lisflood in a post-earthquake mountainous area

Di Wang et al.

Correspondence to: Ming Wang (wangming@bnu.edu.cn)

Content

- **Table S1: History of hazards in the study area.**
- **Figure S1: The generation processes of DEMs (surface DEMs) and bedDEMs (bedrock DEMs). (All the numbers attached to DEM on both sides indicated the corresponding resolution, and the numbers under facilities are the height measured from surface DEM. The numbers in central erodible thickness are the depth of the material, which can be removed by runoff.)**
- **Table S2: The C-L parameter values for the simulations of three scenarios.**
- **Figure S2: The input rainfall series (a and b) and simulation results of the flash flood event in July 2018 (c and d).**
- **Figure S3: The comparison of the simulation results (labelled with a depth range of deposition and inundation in the delimited regions shown in (b)) with images (GF-2 with 8-m resolution, annotated three locations photographed in (c)) and photographic evidence (dimensioned to show the measured results) after the flash flood event in July 2018.**
- **Figure S4: Photos showing the erosion and deposition in different areas: (a) the source area, (b) the deposition area, (c) and (d) the transitional area.**

Table S1: History of hazards in the study area.

Time	Total rainfall (mm)	Details
2008.9.24	140.0	The first post-seismic debris flow occurred in the upriver Mayuanzi. The deposited sediment was up to 5.0×10^4 m^3, resulting in collapsed houses and a mess of farmland in the inundation. *
2009.7.15-7.16	200.0	The debris flow lasted for 20 minutes and carried 2.5×10^4 m^3 solid materials into the outlet section in the catchment. *
2010.8.13	223.3	Loose materials were carried from branch outlets into the main outlet and deposited in their routes. *
2011.8.20	118.0	The scenario was like in 2010.8.13, while damaged less. *
2013.7.7-7.12	800.0	The landslides occurred in the upper steep branch, turning to a rapid and large flow-like motion in the main outlet and sweeping over the houses, pigsty, and arable land near the channel. Eventually, the mixture of soil and fragmented rocks accumulated at 29.5×10^4 m^3. *
2018.7.9-7.11	360.0	A considerable number of sediments were entrained from several branches and the depth of the deposited materials from Qinggangping was more than 2 m on the road.

*devotes to the sources are mainly from literature research (Feng et al., 2017; Guo et al., 2018; Zhao et al., 2019)

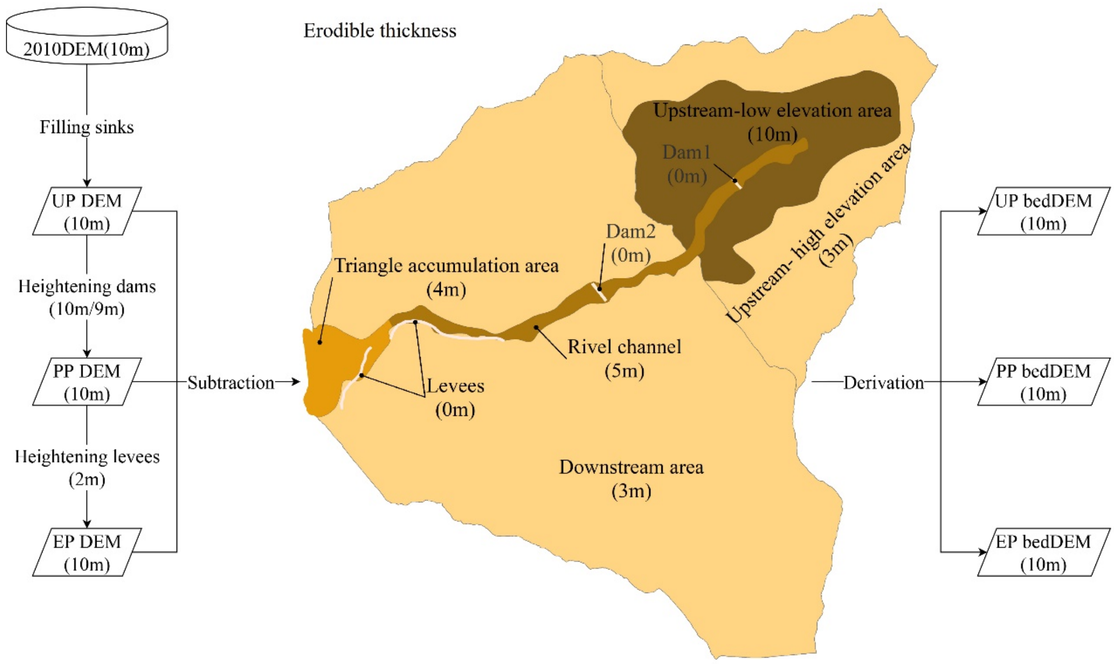

Figure S1: The generation processes of DEMs (surface DEMs) and bedDEMs (bedrock DEMs). (All the numbers attached to DEM on both sides indicated the corresponding resolution, and the numbers under facilities are the height measured from surface DEM. The numbers in central erodible thickness are the depth of the material, which can be removed by runoff.)

Table S2: The C-L parameter values for the simulations of three scenarios.

Parameters	Value	Description
9 kinds of grainsizes (m) (grainsize proportion) ★★	0.000074(0.098), 0.0005(0.138), 0.001(0.052), 0.002(0.162), 0.005(0.158), 0.01(0.169), 0.02(0.13), 0.04(0.06), 0.1(0.033)	Used for calculating the sediment transport in each active layer
Suspended fall velocity(m/s)	0.0003	Designated as the falling velocity for the finest fraction(74µm)
Sediment transport formula ★★★★	Wilcock and Crowe	A criterion calculated the fluvial erosion and deposition for all cells
Max erode limit (m) ★★★	0.002	The maximum amount of material that can be eroded within a cell at each time step
In channel lateral erosion rate ★★★	20	Controlling the channel narrowing
Active layer thickness (m)	0.1	The thickness of a single active layer
Lateral erosion rate ★	0.000003	The variable controls lateral erosion

Lateral edge smoothing passes	40	The number of passes for the edge smoothing filter (distance between two meanders)
Vegetation critical shear stress (Pa) ★★★	100	The value above which vegetation would be removed by fluvial erosion
Grass maturity rate (yr) ★	1	The speed at which vegetation reaches full maturity in years
The proportion of erosion that can occur when vegetation is fully grown	0.1	Determined the effects of vegetation maturity on “in channel lateral erosion rate” and the “lateral erosion rate”.
Soil creep rate(m/yr) ★★	0.0025	The variable tends to cause erosion gradually on sharper features in the terrain
Slope failure threshold (◦) ★★★	60	Angle threshold in degrees above which landslide occur
Input/output difference allowed(m^3/s) ★★	0.5	Described the flow model running in a steady state and used to speed up the model operation
Min Q for depth calculate(m) ★★★	0.1	The value above which the flow depth would be calculated to save running time
Water depth threshold above which erosion will happen(m)	0.01	The value above which the model starts to calculate erosion
The slope for edge cells ★★	0.005	The exit cells’ slope to control the erosion and deposition
Evaporation rate (m/d) ★★★	0.00418	Used to calculate the evapotranspiration
Courant number	0.3	The value controls the numerical stability and speed of operation of the flow model
Manning’s n values (forest, river channel, landslides, farmland, grassland, buildings) ★★	0.07, 0.045, 0.04, 0.035,0.03,0.015	The roughness coefficient used by the flow model

Note: The greater the number of ★, the more sensitive to the model (Skinner et al., 2018).

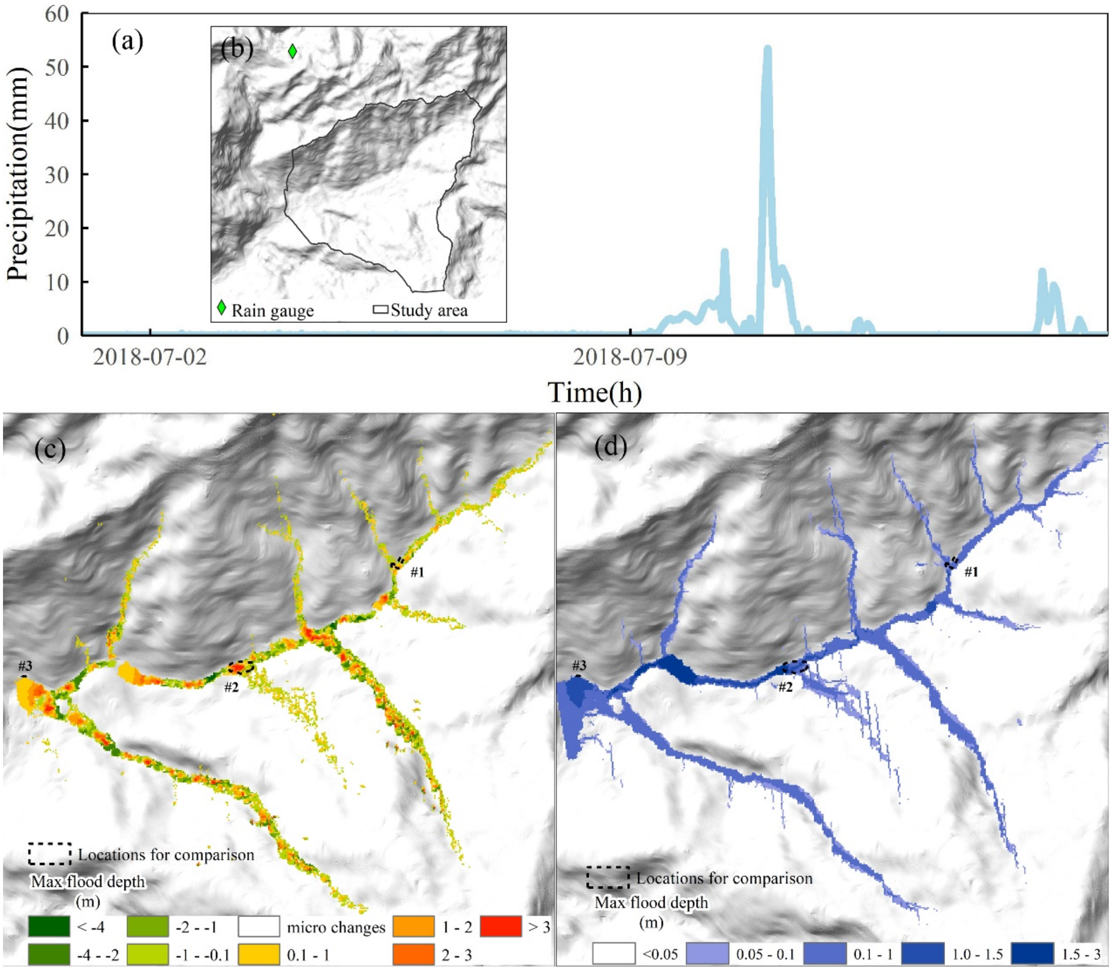

Figure S2: The input rainfall series (a and b) and simulation results of the flash flood event in July 2018 (c and d).

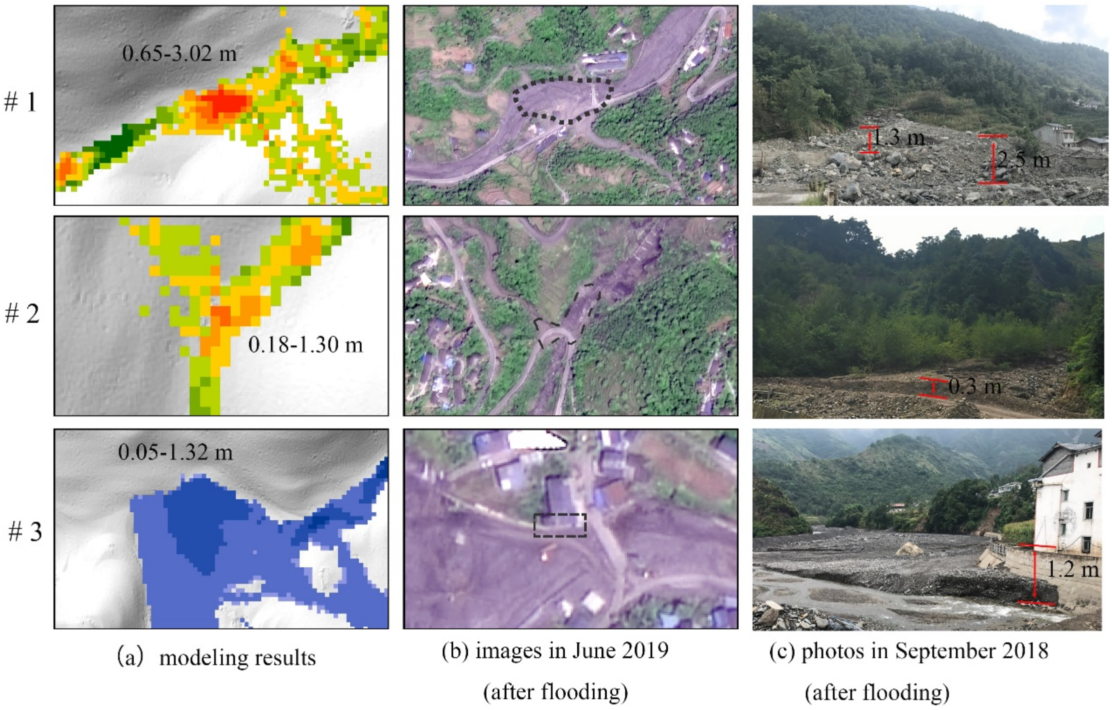

Figure S3: The comparison of the simulation results (labelled with depth range of deposition and

inundation in the delimited regions shown in (b)) with images (GF-2 with 8-m resolution, annotated three locations photographed in (c)) and photographic evidence (dimensioned to show the measured results) after the flash flood event in July 2018.

Figure S4: Photos showing the erosion and deposition in different areas: (a) the source area, (b) the deposition area, (c) and (d) the transitional area.

Reference

Feng, W., He, S., Liu, Z., Yi, X., and Bai, H.: Features of Debris Flows and Their Engineering Control Effects at Xinping Gully of Pingwu County, J. Eng. Geol., 25, 2017.

Guo, Q., Xiao, J., and Guan, X.: The characteristics of debris flow activities and its optimal timing for the control in Shikan River Basin Pingwu Country, Chinese J. Geol. Hazard Control, 29, 2018.

Skinner, C. J., Coulthard, T. J., Schwanghart, W., Van De Wiel, M. J., and Hancock, G.: Global sensitivity analysis of parameter uncertainty in landscape evolution models, Geosci. Model Dev., 11, 4873–4888, https://doi.org/10.5194/gmd-11-4873-2018, 2018.

Zhao, C., Liang, J., Xie, Z., She, T., and Zhang, S.: Remote sensing dynamic analysis of debris flow activity characteristics in strong earthquake area of Wenchuan earthquake 10 years after earthquake-A case study of shikan river watershed of pingwu county, J. Catastrophology, 34, 222–227, https://doi.org/10.3969/j.issn.1000－811X.2019.04.038, 2019.